Cell

The NAD$^+$/Sirtuin Pathway Modulates Longevity through Activation of Mitochondrial UPR and FOXO Signaling

Laurent Mouchiroud,[1,4] Riekelt H. Houtkooper,[1,2,4] Norman Moullan,[1] Elena Katsyuba,[1] Dongryeol Ryu,[1] Carles Cantó,[1,5] Adrienne Mottis,[1] Young-Suk Jo,[1] Mohan Viswanathan,[3] Kristina Schoonjans,[1] Leonard Guarente,[3] and Johan Auwerx[1,*]
[1]Laboratory for Integrative and Systems Physiology, School of Life Sciences, Ecole Polytechnique Fédérale de Lausanne, 1015 Lausanne, Switzerland
[2]Laboratory Genetic Metabolic Diseases, Academic Medical Center, 1105 AZ Amsterdam, The Netherlands
[3]Paul F. Glenn Laboratory, Department of Biology, Massachusetts Institute of Technology, Cambridge, MA 02139, USA
[4]These authors contributed equally to this work
[5]Present address: Nestlé Institute of Health Sciences, 1015 Lausanne, Switzerland
*Correspondence: admin.auwerx@epfl.ch
http://dx.doi.org/10.1016/j.cell.2013.06.016

SUMMARY

NAD$^+$ is an important cofactor regulating metabolic homeostasis and a rate-limiting substrate for sirtuin deacylases. We show that NAD$^+$ levels are reduced in aged mice and *Caenorhabditis elegans* and that decreasing NAD$^+$ levels results in a further reduction in worm lifespan. Conversely, genetic or pharmacological restoration of NAD$^+$ prevents age-associated metabolic decline and promotes longevity in worms. These effects are dependent upon the protein deacetylase *sir-2.1* and involve the induction of mitonuclear protein imbalance as well as activation of stress signaling via the mitochondrial unfolded protein response (UPR^{mt}) and the nuclear translocation and activation of FOXO transcription factor DAF-16. Our data suggest that augmenting mitochondrial stress signaling through the modulation of NAD$^+$ levels may be a target to improve mitochondrial function and prevent or treat age-associated decline.

INTRODUCTION

Alterations in NAD$^+$ levels have a powerful metabolic impact because it serves as an obligatory substrate for the deacetylase activity of the sirtuin proteins (Guarente, 2008; Haigis and Sinclair, 2010; Houtkooper et al., 2010a). The best-characterized mammalian sirtuin is SIRT1, which controls mitochondrial function through the deacetylation of targets that include PGC-1α and FOXO (Chalkiadaki and Guarente, 2012; Houtkooper et al., 2012). The administration of NAD$^+$ precursors, such as nicotinamide mononucleotide (Yoshino et al., 2011) or nicotinamide riboside (NR) (Cantó et al., 2012), has proven to be an efficient way to increase NAD$^+$ levels and SIRT1 activity, improving metabolic homeostasis in mice. Furthermore, the NAD$^+$-consuming poly(ADP-ribose) polymerase proteins—with PARP1 and PARP2 representing the main PARP activities in mammals—were classically described as DNA repair proteins (Gibson and Kraus, 2012; Schreiber et al., 2006), but recent studies have linked these proteins to metabolism (Asher et al., 2010; Bai et al., 2011a, 2011b; Erener et al., 2012). Indeed, genetic or pharmacological inactivation of PARP1 increased tissue NAD$^+$ levels and activated mitochondrial metabolism (Bai et al., 2011b). An association between PARPs and lifespan has been postulated (Grube and Bürkle, 1992; Mangerich et al., 2010), but a causal role remained unclear. A final line of evidence in support of a role for NAD$^+$ in metabolic control came from the deletion of an alternative NAD$^+$-consuming protein, CD38, which also led to NAD$^+$ accumulation and subsequent SIRT1 activation in mice and proved protective against high-fat diet-induced obesity (Barbosa et al., 2007).

Considering the intimate link between metabolism and longevity (Guarente, 2008; Houtkooper et al., 2010b), we hypothesized that increasing NAD$^+$ levels may be sufficient to increase mitochondrial activity and extend lifespan (Houtkooper and Auwerx, 2012). Here, we show how supplementation of PARP inhibitors or NAD$^+$ precursors led to improved mitochondrial homeostasis through the activation of the worm sirtuin homolog, *sir-2.1*. This improvement involved the disturbed balance between OXPHOS subunits encoded by mitochondrial DNA (mtDNA) and nuclear DNA (nDNA), a state we termed mitonuclear protein imbalance. This associates with the activation of the mitochondrial unfolded protein response (UPR^{mt})—a mitochondrial proteostasis pathway promoting longevity (Durieux et al., 2011; Yoneda et al., 2004; Zhao et al., 2002)—and subsequent translocation and activation of the FOXO transcription factor *daf-16*—triggering an antioxidant protection program (Honda and Honda, 1999). Together, our results expose a temporal regulation network for sirtuins on eukaryotic lifespan and pharmacological approaches to control this pathway and prevent age-related physiological decline.

RESULTS

Disturbed NAD$^+$ Metabolism as a Core Biochemical Phenotype of Aging

To establish the role of NAD$^+$ metabolism in aging, we compared PARP activity (global PARylation), NAD$^+$ levels and sirtuin activation in young versus old mice (24 and 103 weeks) (Houtkooper et al., 2011). Both in liver and muscle of aged mice, PARylation was markedly increased (Figure S1A available online). In line with the hypothesis that PARP proteins are major NAD$^+$ consumers, NAD$^+$ levels were robustly decreased in older mice (Figure S1B), confirming recent data (Braidy et al., 2011; Yoshino et al., 2011). Changes in NAD$^+$ are generally translated into altered SIRT1 activity (reviewed in Houtkooper et al., 2012). The lower NAD$^+$ levels in aged mice were indeed reflected in hyperacetylation of the SIRT1 substrate PGC-1α, indicative of reduced SIRT1 activity (Figure S1C). To evaluate the possible contribution of PARP activity and NAD$^+$ metabolism in the aging process, we turned to the worm, *Caenorhabditis elegans*, where it is easier to evaluate the impact of genetic or pharmacological manipulations on lifespan. The aging-associated changes in PARylation and NAD$^+$ levels were evolutionarily conserved as PARylation was also markedly increased with age in nematodes (Figure 1A), and NAD$^+$ levels were lower (Figure 1B). Changes in PARylation and NAD$^+$ were attenuated in worms in which the PARP1 homolog—*pme-1* (Gagnon et al., 2002)—was mutated (Figures 1A and 1B). The residual PARylation is consistent with the presence of a second PARP gene, *pme-2*, which is the worm homolog of the less active PARP2 protein (Cantó and Auwerx, 2012). We further analyzed the natural aging process in worms by monitoring the accumulation of the aging-associated lipid peroxidation product lipofuscin, which was robustly reduced in *pme-1* worms (Figure 1C). We then tested whether reduced NAD$^+$ levels are causally linked to aging. First, we depleted NAD$^+$ chemically using paraquat (Figure 1D), and this is associated with shortened lifespan (Figure 1E). One could argue, however, that the premature death could be caused by excessive DNA damage. Therefore, we also depleted NAD$^+$ genetically. We treated *rrf-3(pk1426)* worms with RNAi targeting *qns-1*, encoding the enzyme NAD$^+$ synthase that catalyzes the final step in NAD$^+$ biosynthesis. Knockdown of *qns-1* indeed depleted NAD$^+$ and shortened lifespan (Figures 1F and 1G). Together, these data suggest that disturbance of the PARP/NAD$^+$-signaling network in aging is evolutionarily conserved and causally involved.

Increasing NAD$^+$ Levels Extends Lifespan through *sir-2.1*

We next aimed to determine whether the age-related NAD$^+$ depletion could be reverted and thereby aging prevented. Strikingly, *pme-1*-deficient worms, either by mutation or RNAi, displayed respectively a 29% or 20% mean lifespan extension (Figure 1H; see Table S1 for statistics). To consolidate these results, we also examined the lifespan of worms upon inhibition of PARP activity with two distinct pan-PARP inhibitors representing different chemical scaffolds (Ferraris, 2010), i.e., AZD2281 (KU59436, olaparib) (Menear et al., 2008), or ABT-888 (veliparib) (Penning et al., 2009). Feeding of worms from eggs until death with different concentrations of PARP inhibitors resulted in a 15%–23% lifespan extension (Figures 1I, 1J, S2A, and S2B; Table S1), with a maximum extension at 100 nM (Figure S2A; Table S2), which is why we chose this concentration for further experiments. Importantly, the lifespan of the *pme-1* mutant was not further extended by AZD2281, confirming that *pme-1* is the major worm PARP activity (Figure 1K).

Besides inhibiting NAD$^+$ breakdown, we also focused on supplying NAD$^+$ precursors, notably the salvage pathway precursors nicotinamide (NAM) and NAM riboside (NR). NAM is the end-product of the sirtuin and PARP reaction, whereas NR is a recently discovered vitamin B3. Both can serve as precursors of NAD (re-)synthesis (reviewed in Houtkooper et al., 2010a). Similar to AZD2281 and ABT-888, lifespan extension was observed when the worms were supplemented with either NAM or NR (Figures 2A and 2B; Table S1). Based on the dose-dependent effects on lifespan (Figures S2C and S2D; Table S2), we selected 500 μM NR and 200 μM NAM as optimal concentrations for further experiments. Importantly, combined supplementation of AZD2281 and NR at their optimal concentration did not synergistically extend lifespan, compared to either compound alone (Figure 2C; Table S1). However, when both compounds were added at a suboptimal dose, each not sufficient to induce longevity (100 μM NR + 10 nM AZD2281), lifespan was synergistically extended (Figure 2D; Table S1).

As observed in *pme-1* worms (Figure 1B), supplementation with PARP inhibitors or NAD$^+$ precursors significantly increased NAD$^+$ levels (Figures 2E, S3A, and S3B). Although the role of SIRT1 or its homologs in lifespan extension under basal, unstressed, conditions is subject of debate (Burnett et al., 2011; Rogina and Helfand, 2004; Tissenbaum and Guarente, 2001; Viswanathan and Guarente, 2011), it holds a central position in healthspan regulation in the context of disease or cellular stress (Houtkooper et al., 2012). Given the NAD$^+$ dependence of sirtuin enzymes (Imai et al., 2000), we analyzed epistasis by treating *sir-2.1(ok434)* mutant worms with the PARP inhibitor AZD2281 or with NR. The effect of both these compounds on longevity was abrogated in the *sir-2.1(ok434)* mutant (Figure 2F), confirming *sir-2.1* dependence of the lifespan extension induced by two distinct strategies to raise NAD$^+$ levels.

PARP Inhibitors and NAD$^+$ Precursors Boost Mitochondrial Function

As NAD$^+$ and SIRT1/*sir-2.1* are thought to influence oxidative metabolism (Guarente, 2008; Houtkooper et al., 2012), we functionally characterized mitochondrial activity in AZD2281- and NR-treated worms by measuring oxygen consumption rates. Although respiration strongly decreased with age in control worms, worms treated with AZD2281, NR, and NAM maintained or even increased respiration at young adult level (Figures 2G and S3C). This was corroborated by increased mitochondrial abundance evaluated by the mtDNA/nDNA ratio (Figure 2H), increased ATP levels (Figure 2I), and increased gene expression of enzymes controlling key metabolic pathways, e.g., the TCA cycle gene citrate synthase (*cts-1*), the glycolysis gene hexokinase (*hxk-1*), and the gluconeogenesis gene pyruvate carboxylase (*pyc-1*) (Figure 2J). Functionally, the improved metabolic state was accompanied by better

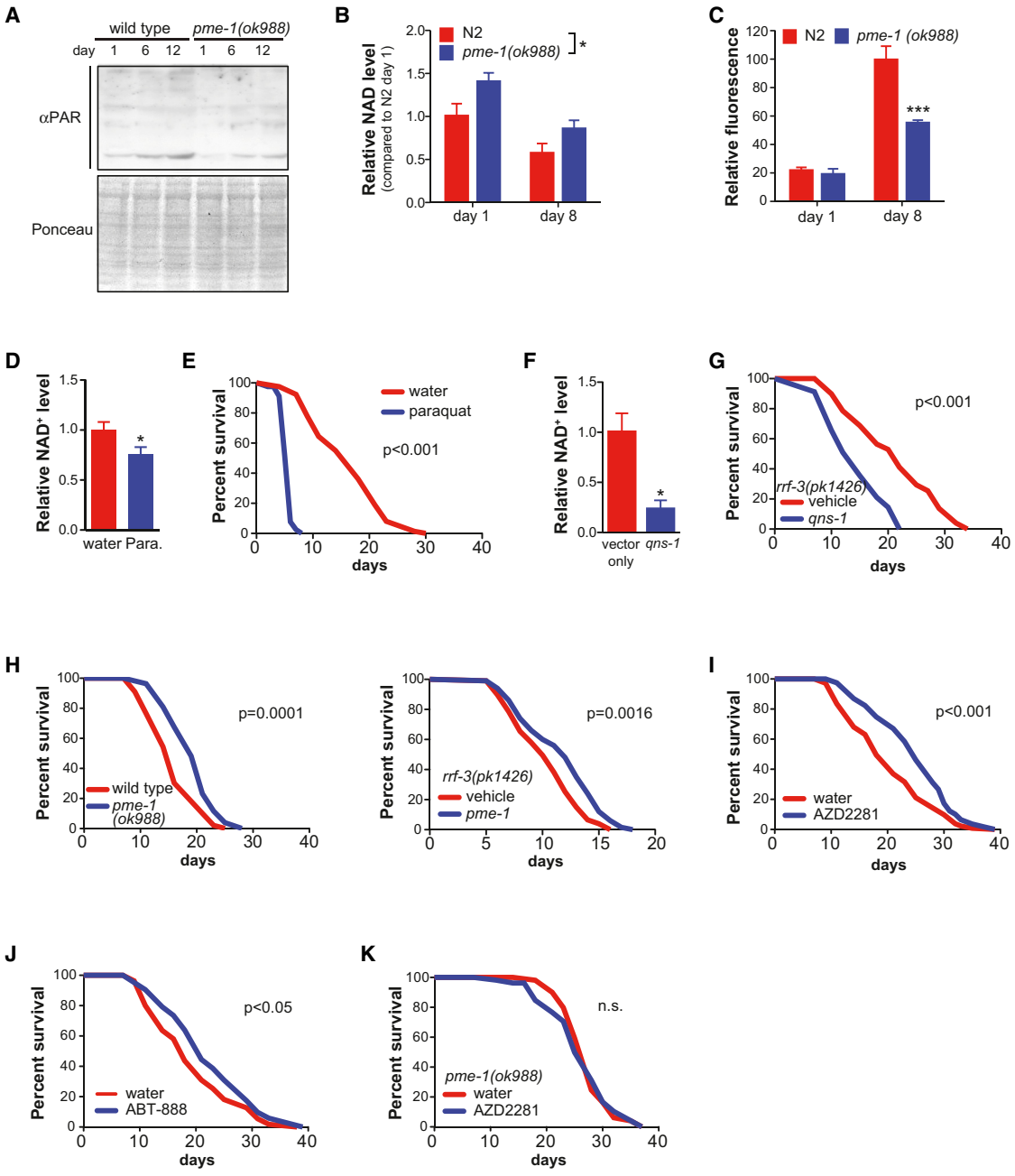

Figure 1. NAD⁺ Is Causally Involved in Aging

(A) Aged *C. elegans* displayed higher total protein PARylation levels, which were largely attenuated in *pme-1* mutants. Ponceau staining is used as a loading control.

(B) Aging decreased worm NAD^+ levels, in both wild-type and in *pme-1* mutant worms, with a higher level of NAD^+ in the *pme-1* mutant during aging. Two-way ANOVA indicated significant difference with age ($p < 0.008$) and genotype ($p = 0.02$).

(C) *pme-1* mutant worms accumulated less of the aging pigment lipofuscin compared to wild-type worms.

(D and E) Supplementation of N2 wild-type worms with 4 mM paraquat depletes NAD^+ levels (D) and shortens lifespan (E).

(F and G) RNAi against *qns-1*, encoding NAD^+ synthase, depletes NAD^+ levels (F) and shortens lifespan in worms (G).

(H) *pme-1(ok988)* mutant worms show a 29% mean lifespan extension (left), whereas *pme-1* RNAi in the *rrf-3(pk1426)* strain extends lifespan by 20% (right).

(I and J) PARP inhibition by either AZD2281 (100 nM) or ABT-888 (100 nM) extended worm lifespan, respectively, by 22.9% (I) and 15% (J).

(K) The lifespan extension of AZD2281 is *pme-1*-dependent.

Bar graphs are expressed as mean ± SEM, *$p \leq 0.05$; **$p \leq 0.01$; ***$p \leq 0.001$. For lifespan curves, p values are shown in the graph (n.s. = not significant). See also Figures S1, S2A, and S2B. See Tables S1 and S2 for additional detail on the lifespan experiments.

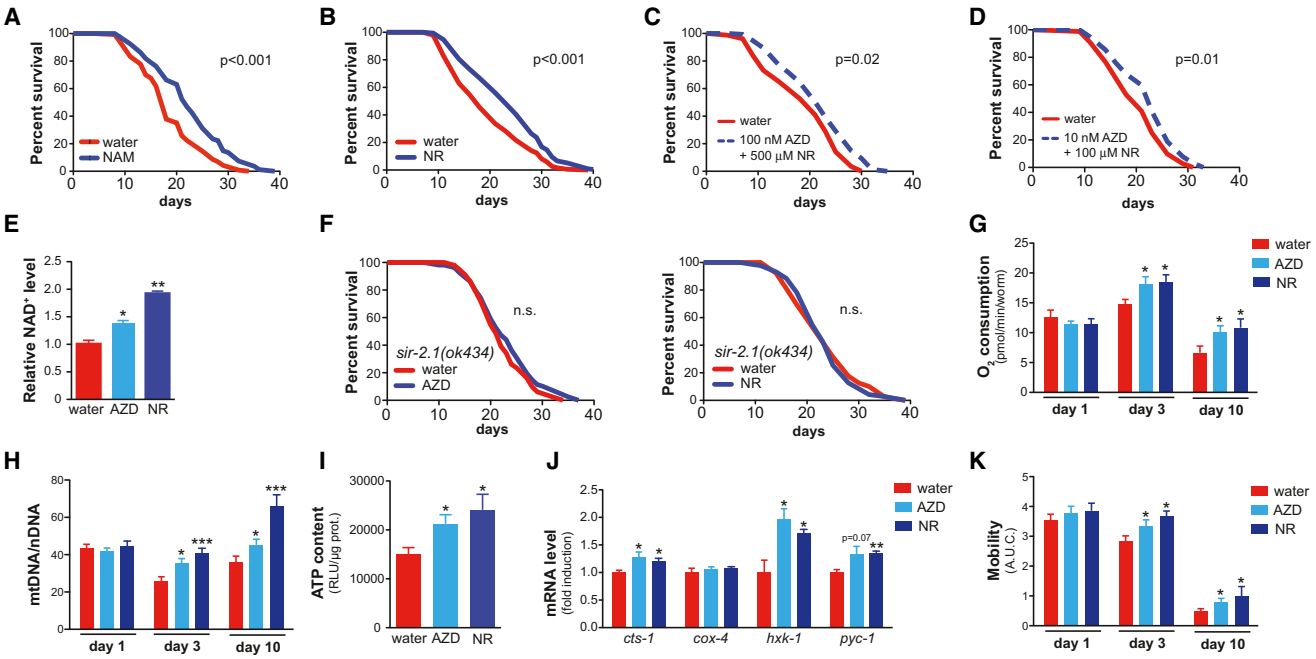

Figure 2. PARP Inhibitors and NAD$^+$ Precursors Increase Mitochondrial Function

(A and B) Supplementation of the NAD$^+$ precursor NR (500 μM; A) or NAM (200 μM; B) in wild-type N2 worms increases lifespan.

(C) Combined treatment using optimal concentrations of AZD2281 (100 nM) and NR (500 μM) extends lifespan (+16%/p = 0.02), but not further than the individual compounds (+22%/p = 0.0004 and +16%/p = 0.01, respectively). Mean lifespans: vehicle: 16.1 ± 0.6 days; 100 nM AZD2281: 19.7 ± 0.8 days; 500 μM NR: 18.7 ± 0.8 days; 100 nM AZD2281+500 μM NR: 18.6 ± 0.7 days.

(D) A combination of sub-optimal doses of AZD2281 (10 nM) and NR (100 μM) extended lifespan (11%/p = 0.01), whereas the individual compounds at these concentrations had no effect on lifespan (+7%/n.s. and +5%/n.s., respectively). Mean lifespans: vehicle: 20.1 ± 0.6 days; 10 nM AZD2281: 21.5 ± 0.7 days; 100 μM NR: 21.1 ± 0.7 days; 10 nM AZD2281+100 μM NR: 22.3 ± 0.7 days.

(E) AZD2281 and NR supplementation increased NAD$^+$ levels in *C. elegans*.

(F) PARP inhibition by AZD2281 (100 nM) and NR supplementation (500 μM) do not extend lifespan in the *sir-2.1(ok434)* mutant (n.s = not significant).

(G) Oxygen consumption was increased in day 3 and day 10 adult worms after AZD2281 (AZD; 100 nM) or NR (500 μM) treatment.

(H) AZD2281 and NR increased mitochondrial biogenesis at day 3 and day 10 of adulthood, as evidenced by the increased mtDNA/nDNA ratio.

(I) AZD2281 and NR increased worm ATP levels at day 3 of adulthood.

(J) AZD2281 and NR increased gene expression (day 3 adults) of key metabolic genes *cts-1* (TCA cycle), *hxk-1* (glycolysis), and *pyc-1* (gluconeogenesis), but not that of *cox-4*.

(K) AZD2281 and NR improved worm fitness at day 3 and 10 of adulthood, as evidenced by measuring worm motility.

Bar graphs are expressed as mean ± SEM, *p ≤ 0.05; **p ≤ 0.01.

See also Figures S2C, S2D, and S3. See Tables S1 and S2 for additional detail on the lifespan experiments.

worm motility at later age (Figure 2K), a sign of improved fitness with age.

Mitochondrial Theories of Aging

Two pathways have been described to link mitochondrial activity and aging, UPR^{mt} and the reactive oxygen species (ROS) defense pathway. UPR^{mt} is activated when protein balance in mitochondria is disturbed. This occurs, for instance, upon accumulation of misfolded or unfolded proteins (Haynes and Ron, 2010). Alternatively, disturbance of the delicate balance between mitochondrial protein production from nDNA and mtDNA—a state we termed mitonuclear protein imbalance—is associated with UPR^{mt} activation (Houtkooper et al., 2013). This triggers a mitochondrial-to-nuclear stress-signaling pathway, which induces the transcription of nDNA-encoded mitochondrial molecular chaperones, such as mtHSP70, HSP60, and HSP10 and the protease CLPP (Durieux et al., 2011; Yoneda et al., 2004; Zhao et al., 2002). On the other hand, the defense against the accumulation of ROS is activated when altered mitochondrial activity causes formation of excessive oxygen radicals, with the ultimate goal of preventing damage of the (sub)cellular microenvironment, e.g., lipids, DNA, and proteins. This pathway involves the nuclear translocation of the FOXO transcription factor *daf-16* (Berdichevsky et al., 2006), which, among other targets, induces the transcription of the mitochondrial antioxidant *sod-3* (Honda and Honda, 1999). The mammalian *daf-16* homolog FOXO3A has been described as a deacetylation target for SIRT1 in mammals (Brunet et al., 2004; Motta et al., 2004; van der Horst et al., 2004), and *daf-16* was shown to interact with *sir-2.1* (Berdichevsky et al., 2006; Hashimoto et al., 2010), providing a possible link between NAD$^+$ and this pathway.

It is unclear whether, and if so how, these two "mitochondrial aging" pathways are activated by NAD$^+$ and how they are intertwined, although it was already shown that ROS do not cause

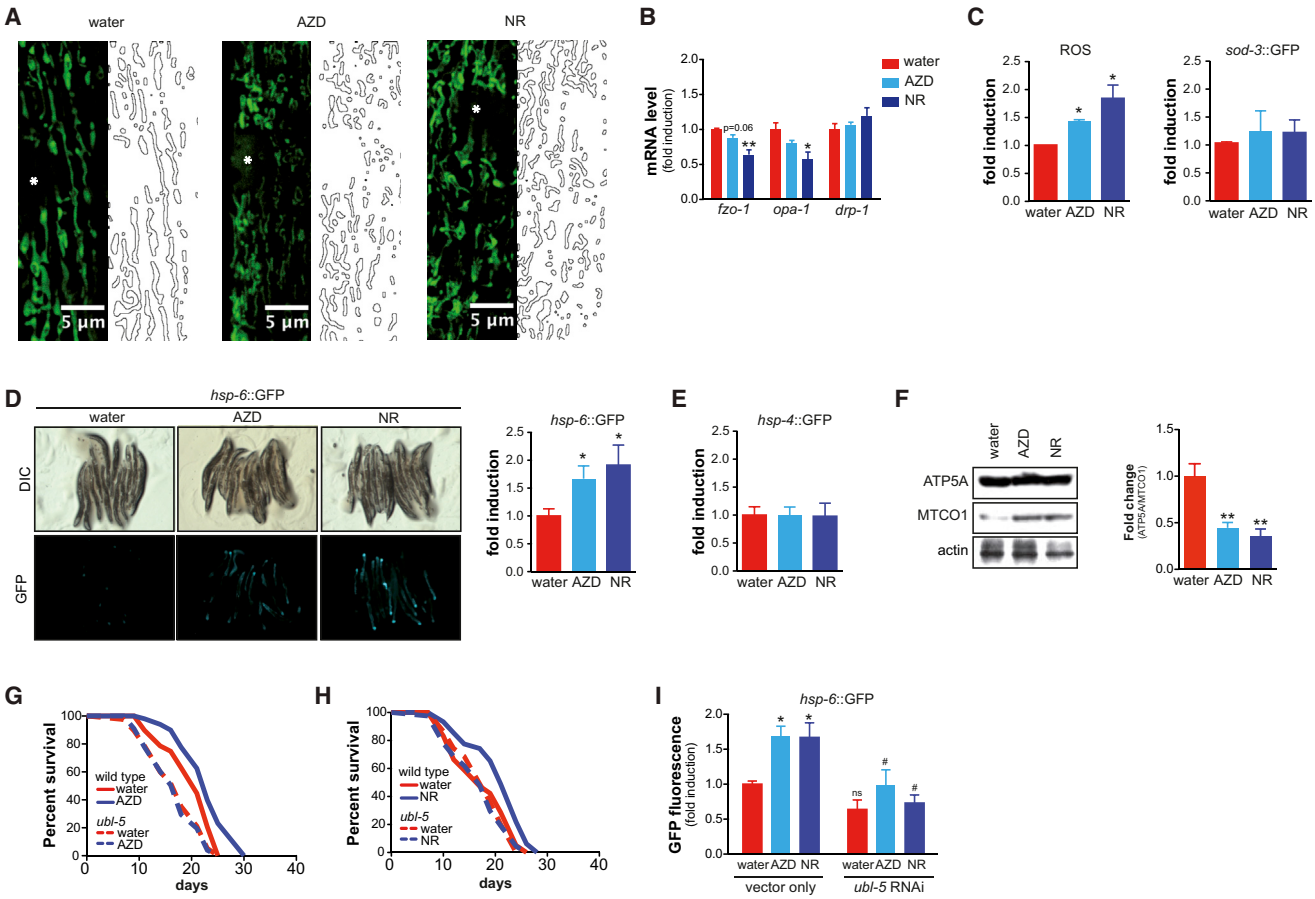

Figure 3. Early Phase Response of NAD$^+$ Boosters on Mitochondrial Aging Pathways

(A) The effects of AZD2281 (100 nM) and NR (500 µM) on mitochondrial content and morphology in body wall muscle. At day 1 of adulthood, mitochondria of AZD2281- or NR-treated worms appear more fragmented. Stars represent nuclei, insets show higher magnification of a small section of the image, marked by dashed rectangle.

(B) At day 1 of adulthood, AZD2281 and NR reduced the expression of mitochondrial fusion genes *fzo-1* and *opa-1*, without affecting the fission gene *drp-1*.

(C) At day 1, AZD2281 and NR cause a burst of ROS, as measured using the MitoSOX probe. This was not accompanied by an induction of the antioxidant gene *sod-3* (measured using a GFP-coupled *sod-3* reporter).

(D and E) At day 1, AZD2281 and NR induced the mitochondrial unfolded protein response (UPR^{mt}) (*hsp-6* reporter; D), without activating the ER unfolded protein response (*hsp-4* reporter; E). In (D), representative images are shown on the left, whereas quantification is shown in the bar graph on the right.

(F) AZD2281 and NR induced mitonuclear protein imbalance, as evidenced by the decreased ratio between nDNA-encoded ATP5A and mtDNA-encoded MTCO1. Representative western blot shown on the left, quantification of the ratio in three independent experiments is shown on the right.

(G and H) RNAi of the UPR^{mt} regulator *ubl-5* abrogated the lifespan extension induced by AZD2281 (G; at 100 nM) and NR (H; at 500 µM).

(I) The UPR^{mt} induction by AZD2281 and NR at day 1 is also *ubl-5*-dependent.

Bar graphs are expressed as mean ± SEM, *p ≤ 0.05; **p ≤ 0.01.

See also Figure S4. See Table S1 for additional detail on the lifespan experiments.

UPR^{mt} (Durieux et al., 2011). We hence set out to perform a detailed temporal analysis of the activation of both stress pathways, focusing on day 1 and day 3 of adulthood. These days were selected based on the premise that they are in different phases of the mitohormesis response (Mouchiroud et al., 2011; Schulz et al., 2007; Zarse et al., 2012). Mitohormesis refers to the concept that an adaptive and protective antioxidant response is activated in mitochondria by an initial accumulation of moderate levels of potentially toxic ROS. Although day 1 is the first day of adulthood and coincides with a burst in ROS production, day 3 is the late reproductive phase (but still pre-aging) and is characterized by activated ROS defense (Schulz et al., 2007).

Early Phase Activation of UPR^{mt} by NAD$^+$ Boosters

By using confocal microscopy in the p*myo-3*::mito::GFP reporter, which expresses mitochondria-targeted GFP in the muscle, we determined the morphology and intensity of the mitochondrial network. At day 1 of adulthood, AZD2281 or NR treatment led to a dense mitochondrial network that appears to be more fragmented compared to vehicle control worms (Figure 3A). This reticular network was likely caused by reduced expression of the mitochondrial fusion genes *fzo-1* and *opa-1*, without changes in the fission regulator *drp-1* (Figure 3B). We then measured the two prime mitochondrial pathways involved in aging, ROS and UPR^{mt}. ROS was measured using

the mitoSOX probe, which indicates specific mitochondrial superoxide production. Both AZD2281 and NR induced a strong superoxide burst at day 1 of adulthood, although at this stage no protective activation of *sod-3* expression was observed (Figure 3C). When we measured at the same age UPR^{mt} activation using *hsp-6*::GFP reporter worms (Yoneda et al., 2004), both compounds robustly induced UPR^{mt} (Figure 3D), without activating the ER-specific unfolded protein response (*hsp-4*::GFP; Figure 3E). Importantly, the induction of UPR^{mt}, but not *sod-3*, was confirmed in worms treated with *pme-1* RNAi, confirming that the effect is not due to off-target effects of the drugs (Figure S4A). The precocious activation of UPR^{mt} after AZD2281 or NR treatment was associated with mitonuclear protein imbalance, as evidenced by the decreased ratio between the nDNA-encoded ATP5A and the mtDNA-encoded MTCO1 (Figure 3F). We next tested whether UPR^{mt} was essential for longevity induced by NAD$^+$ boosters or PARP inhibitors. We used worms treated with RNAi directed against the UPR^{mt} gene, *ubl-5*, an essential component of the mitochondria-to-nucleus feedback (Durieux et al., 2011). Indeed, *ubl-5* RNAi abrogated the lifespan extension conferred by both AZD2281 and NR treatment (Figures 3G and 3H). This coincided with the attenuation of UPR^{mt} activation in *ubl-5* RNAi worms (Figure 3I). These data suggest that UPR^{mt} is an early-phase response induced by increased NAD$^+$ levels.

Late-Phase Activation of ROS Defense by NAD$^+$ Boosters

To test for potential adaptive responses with respect to ROS and UPRmt, we measured similar parameters at day 3 of adulthood. Although fragmented at day 1, mitochondria appear hyperfused at day 3 (Figure 4A), which, at this time, is now associated with increased gene expression of *fzo-1* and *opa-1* (Figure 4B). When we analyzed the activation of UPR^{mt} and ROS defense at day 3 of adulthood, we not only observed a continued activation of UPR^{mt}, but now, unlike the situation at day 1, also a strong activation of the *sod-3* promoter in worms treated with AZD2281, NR (Figure 4C), or *pme-1* RNAi (Figure S4B). We then characterized the ROS defense mechanisms in more detail. At day 3, the higher *sod-3*::GFP levels after AZD2281 or NR treatment were not due to increased *daf-16* gene expression, a key transcriptional regulator of antioxidant defense (Figure 4D). The absence of an induction of the *daf-16* gene suggests that *daf-16* activity might be regulated by AZD2281 and NR via changes in subcellular distribution rather than transcription (Alam et al., 2010). Strikingly, the stress responses were specific for *sod-3* and UPR^{mt}, as expression of cytosolic or ER UPR markers, as well as other antioxidants did not change, or even decrease (Figure 4E).

Considering the strong induction of *sod-3* expression, we next tested whether AZD2281 and NR could protect against the premature aging caused by the ROS-inducer paraquat. Although vehicle-treated worms die young (median = 6 days), AZD2281-, NR-, or NAM-treated worms survive significantly longer (median = 7 days) (Figures 4F and S5A). As mentioned above, DAF-16 activity is primarily regulated by its subcellular localization (Alam et al., 2010). We hence used the *daf-16::*GFP reporter strain to establish DAF-16 localization at day 3 following AZD2281, NR, or NAM exposure. In line with the increased *sod-3* transcriptional activation (Figure 4C), *daf-16* appeared in a more punctate pattern consistent with its nuclear localization that is required for it to activate transcription of its antioxidant target genes (Figures 4G and S5B). Quantitative analysis of this *daf-16* translocation after these various stimuli shows that approximately two to three times more *daf-16* is localized in the nucleus (Figures 4H and S5C). Confirming the crucial role of *daf-16*, we observed that the lifespan extension induced by compounds that enhance NAD$^+$ levels was strictly dependent on the expression of *daf-16* (Figure 4I), suggesting that the induction of antioxidant defense is key for AZD2281 and NR to grant longevity. Finally, the induction of *sod-3* expression was dependent on the presence of the UPR^{mt} regulator *ubl-5* (Figure 4J), suggesting that this UPR^{mt} is involved in the transcriptional activation of antioxidants as well.

UPR^{mt} Controls Lifespan Extension by *sir-2.1* Overexpression

The role of *sir-2.1* in lifespan regulation is debated. Although original reports claimed that overexpression of *sir-2.1* led to strong lifespan extension (Tissenbaum and Guarente, 2001), this was later shown to be partly due to an unlinked mutation affecting sensory perception (Burnett et al., 2011; Viswanathan and Guarente, 2011). Interestingly, when the unintended mutation was lost by genetic outcrossing, the resulting MV389 *sir-2.1* transgenic worm strains maintained an ~10% lifespan extension (Viswanathan and Guarente, 2011). We used this *sir-2.1* transgenic worm strain to test whether increased lifespan due to enhanced sirtuin expression involves UPR^{mt}. The MV389 worms lived 25% longer compared to isogenic controls (Figure 5A) and displayed a robust *sir-2.1* overexpression that could be abrogated using RNAi (Figure 5B). Supplementation of NR in MV389 worms did not further extend lifespan (Figure 5A). The fact that the MV389 worms lived slightly longer in our study compared to previous data (Viswanathan and Guarente, 2011) is due to small differences in our technical approach, as we now censored worms with a protruding vulva phenotype. Similar to compounds that boost NAD$^+$ levels, *sir-2.1* overexpression did not affect the *daf-16* gene expression, but increased expression of mitochondrial regulators *cts-1* and *fzo-1*, the *daf-16* target *sod-3*, and the expression of the UPR^{mt} gene *hsp-6*, without changes in other stress markers, such as *hsp-4*, *hsf-1*, *sod-1*, *sod-2*, *gst-4*, and *prdx-2* (Figure 5C). MV389 worms also displayed mitonuclear protein imbalance with a relative decrease in the ratio between nDNA-encoded ATP5A and mtDNA-encoded MTCO1 (Figure 5D). The longevity of MV389 worms was fully dependent on *sir-2.1* and *daf-16,* as RNAi against these genes completely abrogated the lifespan extension (Figures 5E and 5F). Importantly, *sir-2.1* knockdown in MV389 was also sufficient to block the induction of the UPR^{mt} gene *hsp-6* (Figure 5G). In line with this observation, crossing the *sir-2.1* transgenic worms with the *hsp-6*::GFP UPR^{mt} reporter strain confirmed the robust induction of UPR^{mt} (Figures 5H and 5I), which was attenuated by RNAi targeting *sir-2.1* or the UPR^{mt} regulator *ubl-5* (Figure 5I), indicating an epistatic link between *sir-2.1* expression and the UPR^{mt} pathway. Consistent with this link, *ubl-5* RNAi almost completely restored the lifespan of the MV389 strain to wild-type levels, showing that the effects of *sir-2.1* overexpression were also fully dependent on UPR^{mt} (Figure 5J).

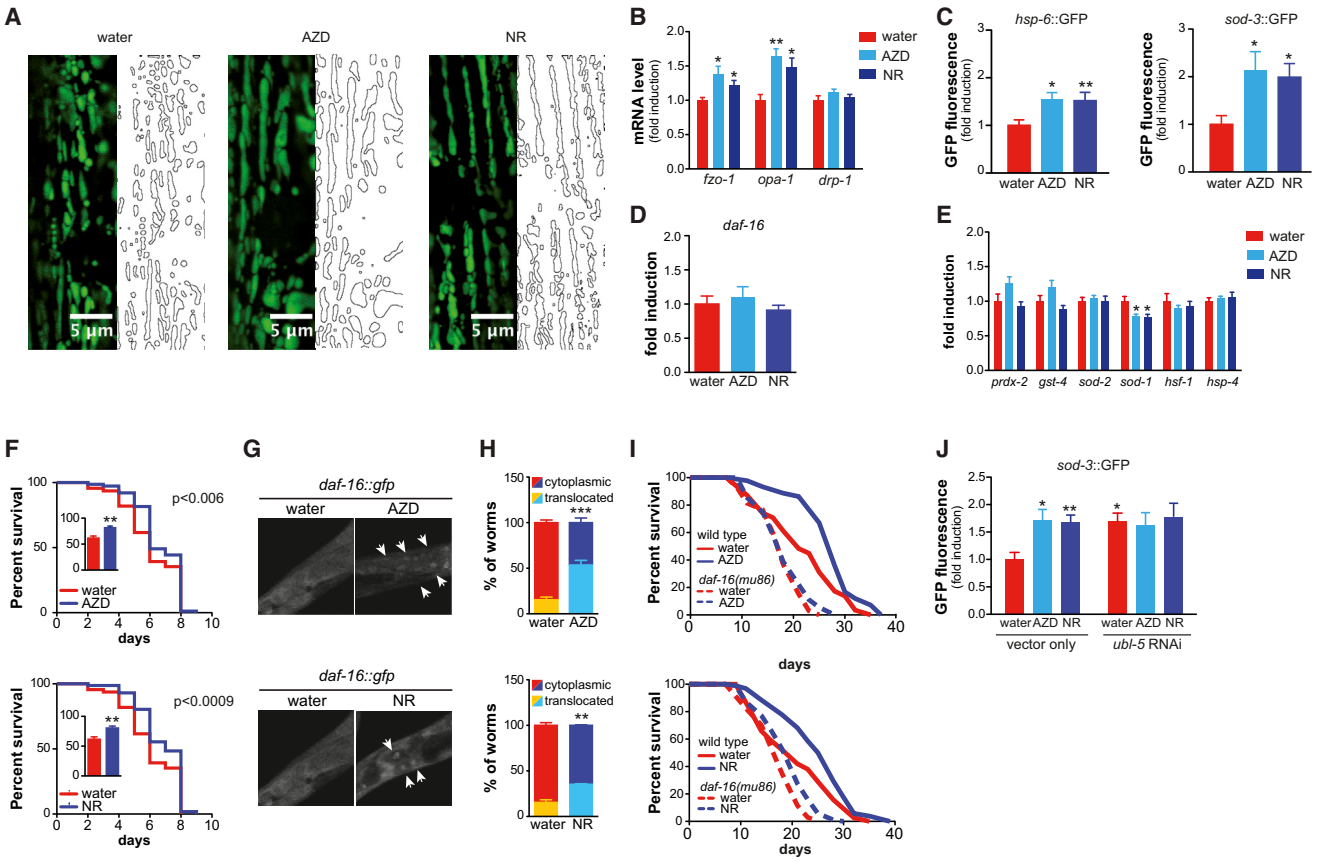

Figure 4. Late-Phase Effects of NAD$^+$ Boosters on Mitochondrial Aging Pathways

(A) The effects of AZD2281 (100 nM) and NR (500 µM) on mitochondrial content and morphology in body wall muscle. At day 3 of adulthood, mitochondria of AZD2281- or NR-treated worms appear more fused. Stars represent nuclei, insets show higher magnification of a small section of the image, marked by dashed rectangle.

(B) At day 3 of adulthood, AZD2281 and NR increased the expression of mitochondrial fusion genes *fzo-1* and *opa-1*, without affecting the fission gene *drp-1*.

(C) At day 3 of AZD2281 (100 nM) or NR (500 µM) treatment, UPR^{mt} is still activated (left), but now accompanied by an induction of the *sod-3*::GFP reporter (right).

(D and E) AZD2281- and NR-treated worms showed no change in *daf-16* expression (D) or activation of expression of other stress genes (E).

(F) Supplementation of PARP inhibitor AZD2281 (100 nM) or NAD$^+$ precursor NR (500 µM) increases mean lifespan of wild-type N2 worms treated with 4 mM paraquat. p Values are shown in the graph.

(G) Representative images of *daf-16*::GFP reporter worms treated with either vehicle or AZD2281 (upper)/NR (lower), showing nuclear accumulation of *daf-16* following treatment, indicated by arrowheads.

(H) Quantification of *daf-16* nuclear translocation following treatment with AZD2281 (upper), NR (lower). Localization is shown as percentage of worms that shows nuclear (yellow or light blue) or cytosolic (red or dark blue) localization.

(I) Lifespan extension following AZD2281 or NR treatment is dependent on *daf-16*.

(J) The induction of *sod-3*::GFP reporter following AZD2281 or NR treatment is dependent on the UPR^{mt} regulator *ubl-5*.

Bar graphs are expressed as mean ± SEM, *p ≤ 0.05; **p ≤ 0.01; ***p ≤ 0.001.

See also Figures S4 and S5. See Table S1 for additional detail on the lifespan experiments.

Increased NAD$^+$/SIRT1 Signaling Induces UPR^{mt} in Mammalian Cells

We next aimed to confirm the physiological relevance of the NAD$^+$/SIRT1/UPR^{mt}/SOD signaling axis in mammalian cells. In line with our previous results in mice (Bai et al., 2011b; Cantó et al., 2012), both PARP inhibition and supplying NAD$^+$ precursors for 48 hr in the hepatocyte cell line AML12 increased the mtDNA/nDNA ratio (Figures 6A and 6B, upper), demonstrating mitochondrial biogenesis. Similar to worms at day 3, biogenesis was accompanied by induction of the mitochondrial fusion gene *Mfn2* (Figures 6A and 6B, lower). Furthermore, AZD2281 and NR dose-dependently induced gene expression of the mammalian UPR^{mt} homolog *Hsp60*, as evidenced using a luciferase reporter controlled by the human *Hsp60* promoter (Figures 6C and 6D). At the protein level, AZD2281 and NR induced the UPR^{mt} protease CLPP (Figures 6E–6H). A detailed time course analyses showed that this UPR^{mt} response was induced after 12 hr (Figures 6E–6H) and coincides with the induction of mitonuclear protein imbalance, reflected by the ratio between nDNA-encoded SDHA versus the mtDNA-encoded MTCO1 (Figures 6E–6H). Interestingly, the expression of SOD2—the mammalian ortholog of worm *sod-3*—also increased, but whereas SOD2 protein

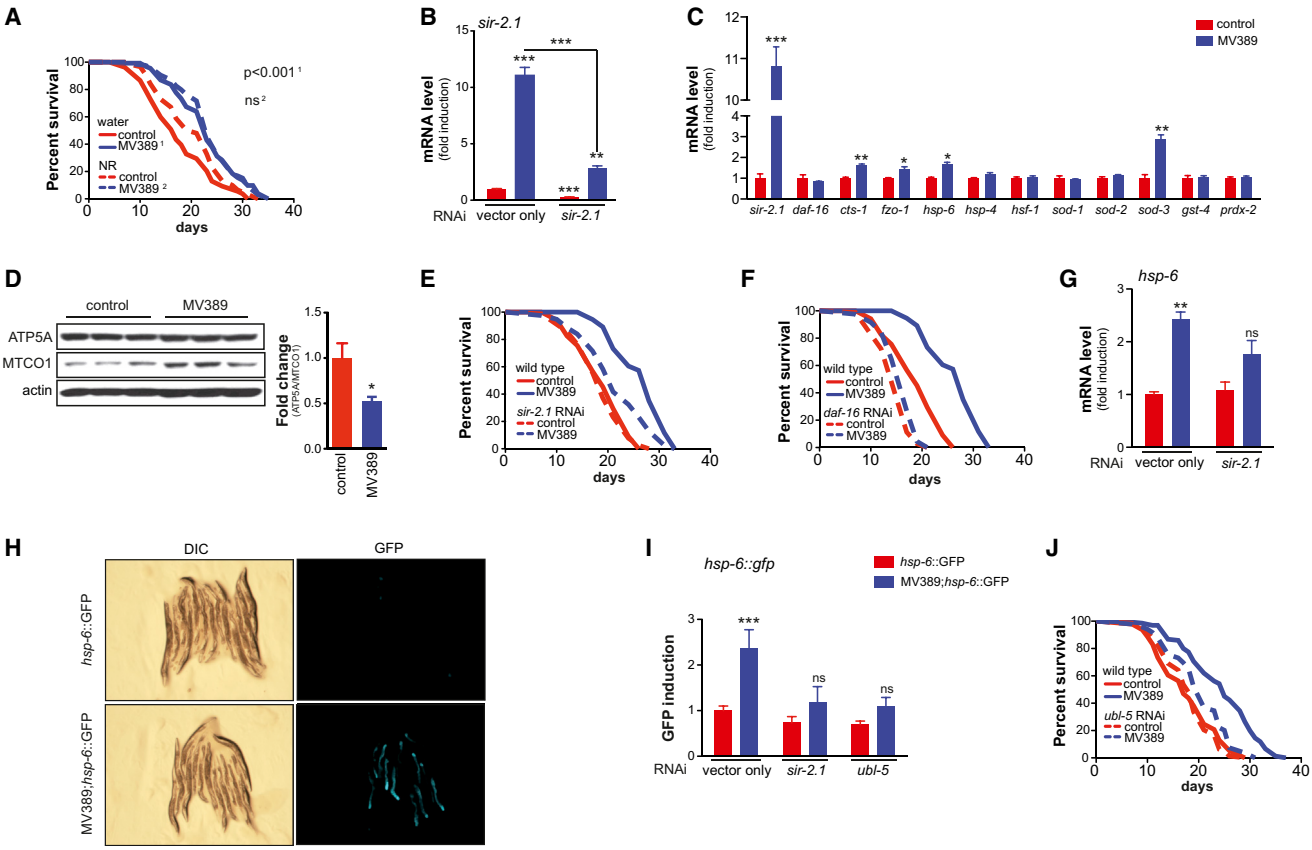

Figure 5. *sir-2.1* Overexpression Extends Lifespan through UPR^{mt}

(A) Outcrossed *sir-2.1* transgenic worms live significantly longer compared to control worms, but NR supplementation does not further extend lifespan. MV389 represents the outcrossed *sir-2.1* overexpressing strain. p Value is shown in the graph.

(B) *sir-2.1* is robustly overexpressed in *sir-2.1* transgenic worms. This induction is almost completely blocked by *sir-2.1* RNAi demonstrating specificity.

(C) *sir-2.1* overexpression induced the gene expression of *cts-1* (TCA cycle), *fzo-1* (mitochondrial fusion), *hsp-6* (UPR^{mt}), and *sod-3* (ROS defense), but not of other stress genes or of the ROS defense regulator *daf-16*.

(D) *sir-2.1* overexpression in MV389-induced mitonuclear protein imbalance, as evidenced by the reduction in the ratio between nDNA-encoded ATP5A and mtDNA-encoded MTCO1. The western blot depicts three independent samples for each strain, whereas the right panel shows a quantification of the mitonuclear protein imbalance.

(E and F) *sir-2.1* (E) and *daf-16* (F) RNAi abrogated the lifespan extension of MV389.

(G) *sir-2.1* overexpression in the MV389 strain induces the UPR^{mt} gene *hsp-6*, an effect that is attenuated upon *sir-2.1* RNAi.

(H and I) In MV389 worms that were crossed with the UPR^{mt} (*hsp-6*::GFP) reporter worms, UPR^{mt} was markedly increased compared to *hsp-6*::GFP control worms. (H) GFP expression in *sir-2.1* wild-type (upper) and *sir-2.1* overexpressing (lower) worms. (I) The quantification of this GFP signal and that this induction was attenuated upon *ubl-5* or *sir-2.1* RNAi.

(J) *ubl-5* RNAi abrogated the lifespan extension of MV389.

Bar graphs are expressed as mean ± SEM, *p ≤ 0.05; **p ≤ 0.01; ***p ≤ 0.001.

See Table S1 for additional detail on the lifespan experiments.

expression trended up 6 hr after starting the treatment (Figures 6E–6H), it was only after 24 hr that both protein level and SOD activity were significantly increased (Figures 6I and 6J), possibly because activity of SOD2 is also regulated by posttranslational modifications such as acetylation (Houtkooper et al., 2012). The late response of SOD2 is reminiscent of the induction of *sod-3* in worms, which is also trailing the primary induction of UPR^{mt} (Figures 3C, 4D, and 4C).

Finally, we assessed mitonuclear protein imbalance and UPR^{mt} activation in primary mouse hepatocytes in which SIRT1 expression was either enhanced or abrogated. Similar to *sir-2.1* transgenic worms, primary hepatocytes in which *Sirt1* was overexpressed by an adenoviral vector (ad-*Sirt1*) showed mitonuclear protein imbalance, i.e., decreased ratio between ATP5A (encoded by nDNA) and MTCO1 (by mtDNA), associated with UPR^{mt} induction—as evidenced by the robust increase in CLPP and HSP60 protein expression—and SOD2 expression, relative to control (Ad-GFP transduced) hepatocytes (Figure 7A). We then aimed to analyze the effect of treating wild-type hepatocytes with AZD2281 or NR, either in the presence or absence of *Sirt1*. To this end, we isolated hepatocytes from floxed *Sirt1* mice (*Sirt1*$^{L2/L2}$). These were subsequently infected with either ad-GFP (for wild-type) or adenoviral-controlled *Cre* recombinase (ad-*Cre*; for *Sirt1* knockout). Similar to ad-*Sirt1*-treated hepatocytes

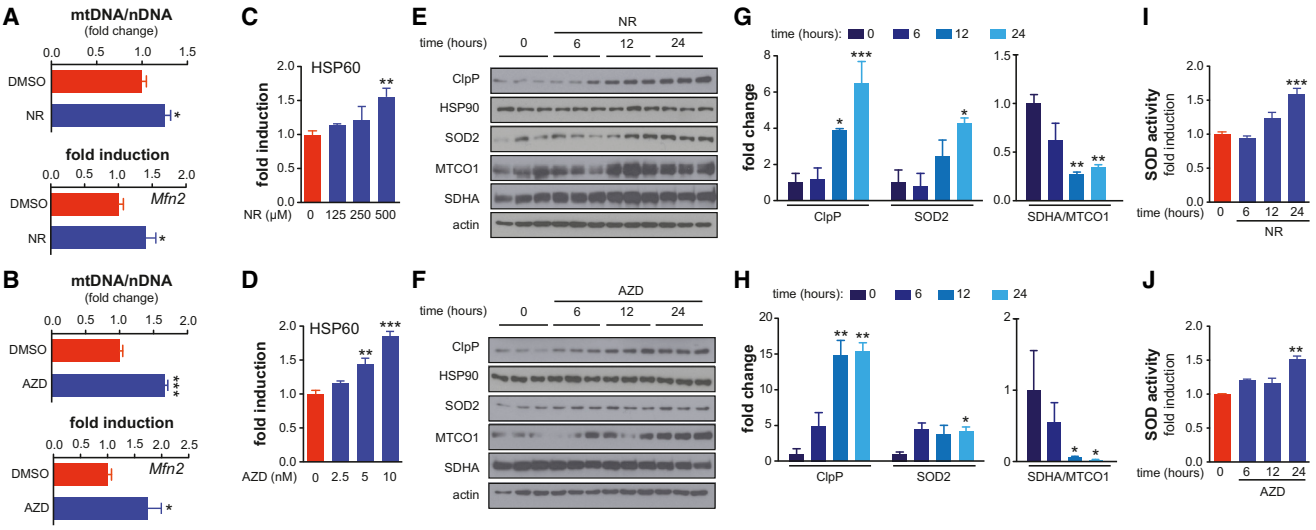

Figure 6. NAD⁺ Boosters Activate UPR^{mt} in Mammalian Cells

(A and B) Treatment with NR (A; 1 mM) or AZD2281 (B; 1 μM) increases the ratio between mitochondrial DNA (mtDNA) and nuclear DNA (nDNA), a common marker for mitochondrial abundance in the AML12 hepatocyte cell line (upper). This increase reflects induced mitochondrial biogenesis. At the same time, NR and AZD2281 induce the expression of the mitochondrial fusion gene *Mfn2* (lower).

(C and D) AZD2281 and NR dose-dependently activate the transcription of a human *Hsp60* promoter luciferase reporter, transfected into AML12 cells.

(E–H) The NAD⁺ precursor NR (E and G; 1 mM) and the PARP inhibitor AZD2281 (F and H; 1 μM) induce UPR^{mt}, as evidenced by CLPP expression, in a time-dependent fashion in AML12 cells. The mitochondrial antioxidant SOD2 also increased over time. HSP90 is a cytosolic stress marker that is not affected by treatment with AZD2281 or NR. NR and AZD2281 also induced marked mitonuclear protein imbalance, as evidenced by the ratio SDHA/MTCO1 (nDNA- and mtDNA-encoded, respectively). Actin served as a loading control. (G and H) Quantifications of the western blots in (E) and (F).

(I and J) At the later stages following NR (I) or AZD2281 (J) treatment, SOD activity was increased. The fact that activity trails behind protein expression may be due to posttranslational modifications regulating SOD2 activity.

Bar graphs are expressed as mean ± SEM, *p ≤ 0.05; **p ≤ 0.01; ***p ≤ 0.001.

(Figure 7A), wild-type primary hepatocytes (ad-GFP) that were treated with AZD2281 or NR displayed mitonuclear protein imbalance—i.e., decreased ratio between nDNA- and mtDNA-encoded OXPHOS proteins—increased UPR^{mt} (CLPP and HSP60) and increased SOD2 expression, whereas these effects were completely blocked in the ad-*Cre* infected *Sirt1* floxed hepatocytes (Figure 7B). Altogether, these data validate the conservation of the NAD⁺/SIRT1/UPR^{mt}/SOD signaling pathway in mammals, as well as the role of mitonuclear protein imbalance therein.

DISCUSSION

The progressive functional decline that happens during the normal aging process is associated with the accumulation of mutations in DNA (Hoeijmakers, 2009) and changes in metabolic rate and mitochondrial function (Houtkooper et al., 2011). How these DNA damage and mitochondrial metabolism pathways are intertwined is starting to be elucidated, but the mechanistic basis remains poorly understood. Key players in both these pathways include the sirtuin and PARP proteins, both NAD⁺-dependent enzymes, and considerable prior knowledge to support a role of these pathways with respect to age-related metabolic diseases has accumulated. For instance, the increased NAD⁺ levels in *Parp1*$^{-/-}$ or *Cd38*$^{-/-}$ mice and in mice treated with the NAD⁺ precursors NR or NMN, led to SIRT1-dependent improved mitochondrial function, protecting them against the metabolic damage induced by high-fat diets (Bai et al., 2011b; Barbosa et al., 2007; Cantó et al., 2012; Yoshino et al., 2011). Conversely, reduced levels of NAD⁺ metabolism were observed in aged rats and mice (Braidy et al., 2011; Yoshino et al., 2011), although no mechanistic explanation of this observation was presented.

We hence set out to investigate the causal link between NAD⁺ and aging, whether increasing NAD⁺ levels and sirtuin activity are sufficient to prevent aging and if so, which downstream aging pathways are involved. We primarily used the nematode *C. elegans* as it allows detailed genetic interventions coupled to full lifespan analysis. Additionally, we set up a range of mammalian, cell-based studies to complement our *C. elegans* results. Our data indicate that PARP activity, by modulating NAD⁺ availability, regulates mitochondrial biogenesis and as such plays an important role to preserve mitochondrial and organismal fitness. Not only is PARylation increased and are NAD⁺ levels reduced in aged worms and mice, but we also show that depleting NAD⁺ levels, either chemically using paraquat or genetically by inhibiting the NAD⁺ synthase *qns-1*, is sufficient to shorten worm lifespan. Conversely, interventions aimed to safeguard NAD⁺ levels curb the aging process and extend lifespan in *C. elegans*. Two independent strategies were used to boost NAD⁺ levels, i.e., mutation/RNAi (*pme-1*) or inhibition (AZD2281 or ABT-888) of the NAD⁺-consuming PARP enzymes and supplementation of NAD⁺ precursors (NR or NAM). The fact that both these approaches to raise NAD⁺ levels promote

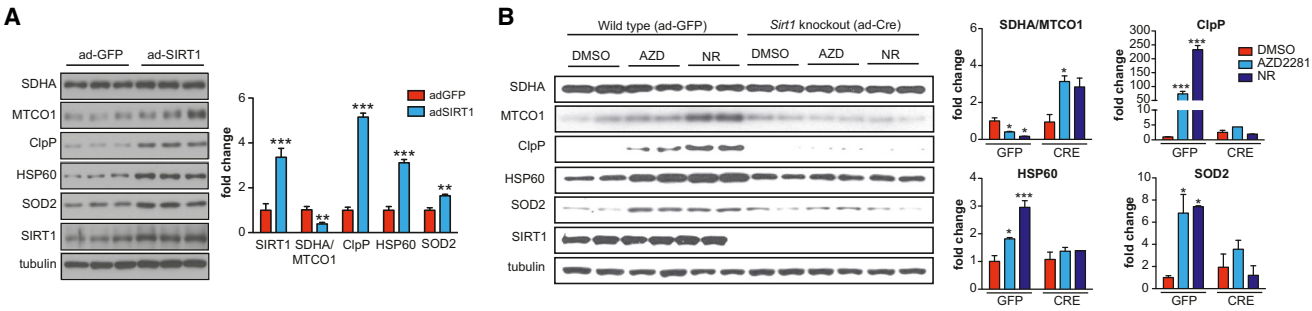

Figure 7. Activation of UPR^{mt} Is *Sirt1* Dependent in Mammals

(A) Primary hepatocytes infected with Ad-m*Sirt1,* to overexpress *Sirt1,* display marked mitonuclear protein imbalance (ratio MTCO1/SDHA), UPR^{mt} activation (CLPP and HSP60), and antioxidant induction (SOD2), compared to hepatocytes from the same isolation infected with Ad-GFP, which served as controls. *Sirt1* overexpression was confirmed; tubulin is used as a loading control.

(B) Primary hepatocytes of *Sirt1* floxed mice were infected with adenoviral-assisted GFP ("wild-type" negative control) or *Cre* recombinase (*Sirt1* knockout). Treatment of GFP controls with NR or AZD2281-induced mitonuclear protein imbalance, and UPR^{mt}, whereas these effects were attenuated when *Sirt1* was knocked out. SIRT1 blots show knockout efficiency; tubulin was probed as a loading control.

Bar graphs are expressed as mean ± SEM, *p ≤ 0.05; **p ≤ 0.01; ***p ≤ 0.001.

See also Figure S6.

a similar phenotype strengthens the hypothesis that NAD$^+$ is a critical metabolite influencing mitochondrial fitness and lifespan in a *sir2.1*-dependent way. Also, because NAD$^+$ precursors and *sir-2.1* overexpression are unlikely to modify the PARylation status of proteins or DNA directly, this excludes PARylation as a causal contributor of aging. Although the role of *sir-2.1* in longevity is subject of debate (reviewed in Houtkooper et al., 2012) our data provide unequivocal evidence in support of its importance in lifespan regulation.

Two aging pathways are known to play a role in the mitochondrial theory of aging, UPR^{mt} and ROS (Durieux et al., 2011; Sena and Chandel, 2012). In worms that accumulated NAD$^+$ or in which *sir-2.1* is overexpressed, we observed a marked induction of UPR^{mt}, as well as improved ROS defense. Based on our time course experiments in worms and its *ubl-5* dependence, we concluded that the initial phase is characterized by a burst in ROS and induction of UPR^{mt}, which is associated with a state we termed mitonuclear protein imbalance, referring to the altered balance between nDNA- and mtDNA-encoded OXPHOS subunits. This suggests that, when nDNA-encoded protein synthesis is not matched by mtDNA-encoded protein synthesis, UPR^{mt} is activated to provide protective capacity. We demonstrated that the UPR^{mt} regulator *ubl-5* is essential for the lifespan extension inferred by either increasing NAD$^+$ levels or by *sir-2.1* overexpression.

Besides UPR^{mt}, the NAD$^+$ boosting strategies, using either the PARP inhibitor AZD2281 or the NAD$^+$ precursors NR and NAM, also induced an antioxidant response. Following an early-phase burst in ROS, DAF-16 translocated to the nucleus, activated expression of the key mitochondrial antioxidant *sod-3*, and likely involves the *sir-2.1/daf-16* signaling pathway (Berdichevsky et al., 2006; Hashimoto et al., 2010). Interestingly, although it was previously shown that ROS are not critically involved in the induction of UPR^{mt} (Durieux et al., 2011), our data demonstrate that the converse may apply, i.e., blocking UPR^{mt} through *ubl-5* RNAi is sufficient to block a further induction the antioxidant response. Although further work is needed to establish how UBL-5 controls *sod-3* expression, the combined activation of UPR^{mt} and ROS defense results in protection against age-related decline and lifespan extension, at least in worms (Figure S6). We confirmed this link also in mammals. PARP inhibitors (Bai et al., 2011b) and NAD$^+$ precursors (Cantó et al., 2012; Yoshino et al., 2011) have been reported to increase NAD$^+$ levels, activate sirtuins and induce mitochondrial biogenesis through PGC-1α in mammals (Cantó et al., 2009; Rodgers et al., 2005). Here, we showed that AZD2281 and NR, but also *Sirt1* overexpression, likewise induced a robust UPR^{mt} and ROS defense in mammals, underscoring the essential and conserved nature of this dual stress response.

Our results expose an evolutionarily conserved pathway by which NAD$^+$/sirtuin activity leads to UPR^{mt}, a SIRT1 signaling pathway, that in parallel to the established *daf-16/sod-3* antioxidant defense (Berdichevsky et al., 2006), improves metabolic health and extends lifespan. We expect that other sirtuin activating compounds may also induce UPR^{mt}. Indeed, data from our lab indicates that resveratrol requires UPR^{mt} activation to extend lifespan (Houtkooper et al., 2013). Altogether, the data in the worm assembled in this study validate a link between NAD$^+$, sirtuins, UPR^{mt}, antioxidants, and lifespan control. Furthermore, our results in mammalian cell-based systems suggest that the mechanisms underlying NAD$^+$/SIRT1/UPR^{mt}/SOD signaling pathway are conserved and may open up the opportunity for preventive and/or therapeutic use of this pathway in the context of aging and aging-related disorders.

EXPERIMENTAL PROCEDURES

C. elegans Experiments

C. elegans strains were cultured at 20°C on nematode growth media agar plates seeded with *Escherichia coli* strain OP50 unless stated otherwise. Strains were provided by the *Caenorhabditis* Genetics Center (University of Minnesota) and detailed in the Extended Experimental Procedures. Worm lifespan tests were performed as described (Mouchiroud et al., 2011). Briefly, 60–100 animals were used per conditions and scored every other day.

Treatments with PARP inhibitors—AZD2281 and ABT-888—or NAD^+ precursors—nicotinamide riboside (NR) and nicotinamide (NAM)—were added at the indicated concentration just before pouring the plates. Animals were exposed to compounds during the full life from eggs until death.

Mammalian Experiments

Primary hepatocytes were isolated from *Sirt1*$^{L2/L2}$ (see more details in Extended Experimental Procedures) and transduced either with an Ad-GFP or an Ad-Cre virus at a MOI = 5 to generate matched *Sirt1*$^{+/+}$ (wild-type) and *Sirt1*$^{-/-}$ (knockout) hepatocytes, respectively. After overnight infection, culture medium was removed and *Sirt1*$^{+/+}$ and *Sirt1*$^{-/-}$ hepatocytes cultures were treated or not with NR or AZD2281. To obtain gain-of-Sirt1-function hepatocytes, Ad-mSirt1 (adgene 8438) or Ad-GFP virus was used at the same MOI to infect primary hepatocytes obtained from a male C57BL/6J mouse to generate hepatocytes overexpressing *Sirt1* and GFP (control hepatocytes), respectively. Mouse experiments were performed in accordance with Swiss law and institutional guidelines.

Worm- and Cell-Based Assays

Worm oxygen consumption was measured using the Seahorse XF96 equipment (Seahorse Bioscience). Worms were transferred in 96-well standard Seahorse plates (ten worms/well) and oxygen consumption was measured six times. Respiration rates were normalized to the number of worms in each individual well. Gene expression (RT-qPCR, primer sequences in Table S3), protein expression (western blot), mtDNA copy number, and ROS assays were performed following routine procedures, as outlined in the Extended Experimental Procedures.

Statistics

Survival analyses were performed using the Kaplan-Meier method and the significance of differences between survival curves calculated using the log rank test. Differences between two groups were assessed using two-tailed t tests. To compare the interaction between age and genotype, two-way ANOVA tests were performed. Analysis of variance, assessed by Bonferroni multiple comparison test, was used when comparing more than two groups. We used R (R software version 2.9.0) for the calculation of mean lifespan and SEM and GraphPad Prism 5 (GraphPad Software) for all other statistical analyses. All p values < 0.05 were considered significant.

SUPPLEMENTAL INFORMATION

Supplemental Information includes Extended Experimental Procedures, six figures, and three tables, and can be found with this article online at http://dx.doi.org/10.1016/j.cell.2013.06.016.

ACKNOWLEDGMENTS

We thank Pierre Gönczy for sharing reagents and equipment, the *Caenorhabditis* Genetics Center for providing worm strains, and the Auwerx team for discussions. L.M. is supported by the "Fondation pour la Recherche Médicale" and R.H.H. by a VENI grant from ZonMw (number 91613050) and an AMC postdoctoral fellowship. J.A. is the Nestlé Chair in Energy Metabolism. This work is supported by grants from the Ecole Polytechnique Fédérale de Lausanne, EU Ideas program (ERC-2008-AdG-23138), NIH (R01HL106511-01A and R01AG043930), Velux Stiftung, and Swiss National Science Foundation (31003A-124713, 31003A-125487, and CSRII3-136201).

Received: November 15, 2012
Revised: April 25, 2013
Accepted: June 11, 2013
Published: July 18, 2013

REFERENCES

Alam, H., Williams, T.W., Dumas, K.J., Guo, C., Yoshina, S., Mitani, S., and Hu, P.J. (2010). EAK-7 controls development and life span by regulating nuclear DAF-16/FoxO activity. Cell Metab. *12*, 30–41.

Asher, G., Reinke, H., Altmeyer, M., Gutierrez-Arcelus, M., Hottiger, M.O., and Schibler, U. (2010). Poly(ADP-ribose) polymerase 1 participates in the phase entrainment of circadian clocks to feeding. Cell *142*, 943–953.

Bai, P., Canto, C., Brunyánszki, A., Huber, A., Szántó, M., Cen, Y., Yamamoto, H., Houten, S.M., Kiss, B., Oudart, H., et al. (2011a). PARP-2 regulates SIRT1 expression and whole-body energy expenditure. Cell Metab. *13*, 450–460.

Bai, P., Cantó, C., Oudart, H., Brunyánszki, A., Cen, Y., Thomas, C., Yamamoto, H., Huber, A., Kiss, B., Houtkooper, R.H., et al. (2011b). PARP-1 inhibition increases mitochondrial metabolism through SIRT1 activation. Cell Metab. *13*, 461–468.

Barbosa, M.T., Soares, S.M., Novak, C.M., Sinclair, D., Levine, J.A., Aksoy, P., and Chini, E.N. (2007). The enzyme CD38 (a NAD glycohydrolase, EC 3.2.2.5) is necessary for the development of diet-induced obesity. FASEB J. *21*, 3629–3639.

Berdichevsky, A., Viswanathan, M., Horvitz, H.R., and Guarente, L. (2006). C. elegans SIR-2.1 interacts with 14-3-3 proteins to activate DAF-16 and extend life span. Cell *125*, 1165–1177.

Braidy, N., Guillemin, G.J., Mansour, H., Chan-Ling, T., Poljak, A., and Grant, R. (2011). Age related changes in NAD+ metabolism oxidative stress and Sirt1 activity in Wistar rats. PLoS ONE *6*, e19194.

Brunet, A., Sweeney, L.B., Sturgill, J.F., Chua, K.F., Greer, P.L., Lin, Y., Tran, H., Ross, S.E., Mostoslavsky, R., Cohen, H.Y., et al. (2004). Stress-dependent regulation of FOXO transcription factors by the SIRT1 deacetylase. Science *303*, 2011–2015.

Burnett, C., Valentini, S., Cabreiro, F., Goss, M., Somogyvári, M., Piper, M.D., Hoddinott, M., Sutphin, G.L., Leko, V., McElwee, J.J., et al. (2011). Absence of effects of Sir2 overexpression on lifespan in C. elegans and Drosophila. Nature *477*, 482–485.

Cantó, C., and Auwerx, J. (2012). Targeting sirtuin 1 to improve metabolism: all you need is NAD(+)? Pharmacol. Rev. *64*, 166–187.

Cantó, C., Gerhart-Hines, Z., Feige, J.N., Lagouge, M., Noriega, L., Milne, J.C., Elliott, P.J., Puigserver, P., and Auwerx, J. (2009). AMPK regulates energy expenditure by modulating NAD+ metabolism and SIRT1 activity. Nature *458*, 1056–1060.

Cantó, C., Houtkooper, R.H., Pirinen, E., Youn, D.Y., Oosterveer, M.H., Cen, Y., Fernandez-Marcos, P.J., Yamamoto, H., Andreux, P.A., Cettour-Rose, P., et al. (2012). The NAD(+) precursor nicotinamide riboside enhances oxidative metabolism and protects against high-fat diet-induced obesity. Cell Metab. *15*, 838–847.

Chalkiadaki, A., and Guarente, L. (2012). Sirtuins mediate mammalian metabolic responses to nutrient availability. Nat. Rev. Endocrinol. *8*, 287–296.

Durieux, J., Wolff, S., and Dillin, A. (2011). The cell-non-autonomous nature of electron transport chain-mediated longevity. Cell *144*, 79–91.

Erener, S., Mirsaidi, A., Hesse, M., Tiaden, A.N., Ellingsgaard, H., Kostadinova, R., Donath, M.Y., Richards, P.J., and Hottiger, M.O. (2012). ARTD1 deletion causes increased hepatic lipid accumulation in mice fed a high-fat diet and impairs adipocyte function and differentiation. FASEB J. *26*, 2631–2638.

Ferraris, D.V. (2010). Evolution of poly(ADP-ribose) polymerase-1 (PARP-1) inhibitors. From concept to clinic. J. Med. Chem. *53*, 4561–4584.

Gagnon, S.N., Hengartner, M.O., and Desnoyers, S. (2002). The genes pme-1 and pme-2 encode two poly(ADP-ribose) polymerases in Caenorhabditis elegans. Biochem. J. *368*, 263–271.

Gibson, B.A., and Kraus, W.L. (2012). New insights into the molecular and cellular functions of poly(ADP-ribose) and PARPs. Nat. Rev. Mol. Cell Biol. *13*, 411–424.

Grube, K., and Bürkle, A. (1992). Poly(ADP-ribose) polymerase activity in mononuclear leukocytes of 13 mammalian species correlates with species-specific life span. Proc. Natl. Acad. Sci. USA *89*, 11759–11763.

Guarente, L. (2008). Mitochondria—a nexus for aging, calorie restriction, and sirtuins? Cell *132*, 171–176.

Haigis, M.C., and Sinclair, D.A. (2010). Mammalian sirtuins: biological insights and disease relevance. Annu. Rev. Pathol. *5*, 253–295.

Hashimoto, T., Horikawa, M., Nomura, T., and Sakamoto, K. (2010). Nicotinamide adenine dinucleotide extends the lifespan of Caenorhabditis elegans mediated by sir-2.1 and daf-16. Biogerontology *11*, 31–43.

Haynes, C.M., and Ron, D. (2010). The mitochondrial UPR - protecting organelle protein homeostasis. J. Cell Sci. *123*, 3849–3855.

Hoeijmakers, J.H. (2009). DNA damage, aging, and cancer. N. Engl. J. Med. *361*, 1475–1485.

Honda, Y., and Honda, S. (1999). The daf-2 gene network for longevity regulates oxidative stress resistance and Mn-superoxide dismutase gene expression in Caenorhabditis elegans. FASEB J. *13*, 1385–1393.

Houtkooper, R.H., and Auwerx, J. (2012). Exploring the therapeutic space around NAD+. J. Cell Biol. *199*, 205–209.

Houtkooper, R.H., Cantó, C., Wanders, R.J., and Auwerx, J. (2010a). The secret life of NAD+: an old metabolite controlling new metabolic signaling pathways. Endocr. Rev. *31*, 194–223.

Houtkooper, R.H., Williams, R.W., and Auwerx, J. (2010b). Metabolic networks of longevity. Cell *142*, 9–14.

Houtkooper, R.H., Argmann, C., Houten, S.M., Canto, C., Jeninga, E.H., Andreux, P.A., Thomas, C., Doenlen, R., Schoonjans, K., and Auwerx, J. (2011). The metabolic footprint of aging in mice. Sci. Rep. *1*, 134.

Houtkooper, R.H., Pirinen, E., and Auwerx, J. (2012). Sirtuins as regulators of metabolism and healthspan. Nat. Rev. Mol. Cell Biol. *13*, 225–238.

Houtkooper, R.H., Mouchiroud, L., Ryu, D., Moullan, N., Katsyuba, E., Knott, G., Williams, R.W., and Auwerx, J. (2013). Mitonuclear protein imbalance as a conserved longevity mechanism. Nature *497*, 451–457.

Imai, S., Armstrong, C.M., Kaeberlein, M., and Guarente, L. (2000). Transcriptional silencing and longevity protein Sir2 is an NAD-dependent histone deacetylase. Nature *403*, 795–800.

Mangerich, A., Herbach, N., Hanf, B., Fischbach, A., Popp, O., Moreno-Villanueva, M., Bruns, O.T., and Bürkle, A. (2010). Inflammatory and age-related pathologies in mice with ectopic expression of human PARP-1. Mech. Ageing Dev. *131*, 389–404.

Menear, K.A., Adcock, C., Boulter, R., Cockcroft, X.L., Copsey, L., Cranston, A., Dillon, K.J., Drzewiecki, J., Garman, S., Gomez, S., et al. (2008). 4-[3-(4-cyclopropanecarbonylpiperazine-1-carbonyl)-4-fluorobenzyl]-2H-phthalazin-1-one: a novel bioavailable inhibitor of poly(ADP-ribose) polymerase-1. J. Med. Chem. *51*, 6581–6591.

Motta, M.C., Divecha, N., Lemieux, M., Kamel, C., Chen, D., Gu, W., Bultsma, Y., McBurney, M., and Guarente, L. (2004). Mammalian SIRT1 represses forkhead transcription factors. Cell *116*, 551–563.

Mouchiroud, L., Molin, L., Kasturi, P., Triba, M.N., Dumas, M.E., Wilson, M.C., Halestrap, A.P., Roussel, D., Masse, I., Dallière, N., et al. (2011). Pyruvate imbalance mediates metabolic reprogramming and mimics lifespan extension by dietary restriction in Caenorhabditis elegans. Aging Cell *10*, 39–54.

Penning, T.D., Zhu, G.D., Gandhi, V.B., Gong, J., Liu, X., Shi, Y., Klinghofer, V., Johnson, E.F., Donawho, C.K., Frost, D.J., et al. (2009). Discovery of the Poly(ADP-ribose) polymerase (PARP) inhibitor 2-[(R)-2-methylpyrrolidin-2-yl]-1H-benzimidazole-4-carboxamide (ABT-888) for the treatment of cancer. J. Med. Chem. *52*, 514–523.

Rodgers, J.T., Lerin, C., Haas, W., Gygi, S.P., Spiegelman, B.M., and Puigserver, P. (2005). Nutrient control of glucose homeostasis through a complex of PGC-1alpha and SIRT1. Nature *434*, 113–118.

Rogina, B., and Helfand, S.L. (2004). Sir2 mediates longevity in the fly through a pathway related to calorie restriction. Proc. Natl. Acad. Sci. USA *101*, 15998–16003.

Schreiber, V., Dantzer, F., Ame, J.C., and de Murcia, G. (2006). Poly(ADP-ribose): novel functions for an old molecule. Nat. Rev. Mol. Cell Biol. *7*, 517–528.

Schulz, T.J., Zarse, K., Voigt, A., Urban, N., Birringer, M., and Ristow, M. (2007). Glucose restriction extends Caenorhabditis elegans life span by inducing mitochondrial respiration and increasing oxidative stress. Cell Metab. *6*, 280–293.

Sena, L.A., and Chandel, N.S. (2012). Physiological roles of mitochondrial reactive oxygen species. Mol. Cell *48*, 158–167.

Tissenbaum, H.A., and Guarente, L. (2001). Increased dosage of a sir-2 gene extends lifespan in Caenorhabditis elegans. Nature *410*, 227–230.

van der Horst, A., Tertoolen, L.G., de Vries-Smits, L.M., Frye, R.A., Medema, R.H., and Burgering, B.M. (2004). FOXO4 is acetylated upon peroxide stress and deacetylated by the longevity protein hSir2(SIRT1). J. Biol. Chem. *279*, 28873–28879.

Viswanathan, M., and Guarente, L. (2011). Regulation of Caenorhabditis elegans lifespan by sir-2.1 transgenes. Nature *477*, E1–E2.

Yoneda, T., Benedetti, C., Urano, F., Clark, S.G., Harding, H.P., and Ron, D. (2004). Compartment-specific perturbation of protein handling activates genes encoding mitochondrial chaperones. J. Cell Sci. *117*, 4055–4066.

Yoshino, J., Mills, K.F., Yoon, M.J., and Imai, S. (2011). Nicotinamide mononucleotide, a key NAD(+) intermediate, treats the pathophysiology of diet- and age-induced diabetes in mice. Cell Metab. *14*, 528–536.

Zarse, K., Schmeisser, S., Groth, M., Priebe, S., Beuster, G., Kuhlow, D., Guthke, R., Platzer, M., Kahn, C.R., and Ristow, M. (2012). Impaired insulin/IGF1 signaling extends life span by promoting mitochondrial L-proline catabolism to induce a transient ROS signal. Cell Metab. *15*, 451–465.

Zhao, Q., Wang, J., Levichkin, I.V., Stasinopoulos, S., Ryan, M.T., and Hoogenraad, N.J. (2002). A mitochondrial specific stress response in mammalian cells. EMBO J. *21*, 4411–4419.